

Statistical Equilibria of Uniformly Forced Advection Condensation

Jai Sukhatme¹ and Raymond T. Pierrehumbert²¹ Mathematics Department, University of Wisconsin-Madison, Madison, WI 53706² Department of Geophysical Sciences, University of Chicago, Chicago, IL 60637
(Dated: January 26, 2020)

We examine the state of statistical equilibrium attained by a uniformly forced condensable substance subjected to advection in a periodic domain. In particular, working in the limit of rapid condensation we study the probability density function (PDF) of the condensable field whenever the advecting velocity field admits a diffusive representation in the equation governing evolution of probability. Following a peak at small values of the condensable field, the derived PDF decays exponentially before terminating in a rapid "roll-off" near saturation. Possible physical implications of this feature as compared to a PDF which continues to decay slowly are pointed out. A set of simple numerical exercises which employ lattice maps for purposes of advection are performed to test these features. Despite the simplicity of the model, the derived PDF is seen to compare favourably with PDF's constructed from isentropic specific humidity data. Further, structure functions associated with the condensable field are seen to scale anomalously with near saturation of the scaling exponents for high moments — a feature which agrees with studies of high resolution aircraft data.

PACS numbers: PACS number 47.52.+j, 05.45.-a

I. INTRODUCTION

Advection-Diffusion-Condensation (ADC) is a variant of the familiar passive advection-diffusion problem [1], wherein apart from molecular diffusion a tracer is subject to an additional sink associated with the process of condensation. A study of the interplay of these processes is motivated by the need to understand the large scale distribution of water vapor in the troposphere [2],[3],[4]. Indeed, the prominent role played by water vapor in various problems related to the Earth's climate [5] — for example, via the water vapor feedback in the greenhouse effect [6] — makes this an important issue. In this context, ADC serves as an idealized problem for water vapor in the troposphere [7]. The mixing ratio $q(\mathbf{x};t)$ of a scalar tracer subject to advection, diffusion and condensation is governed by

$$\frac{\partial q}{\partial t} + (\mathbf{u} \cdot \nabla)q = -r^2 q + S(q; q_s) + F \quad (1)$$

here \mathbf{u} and F are the advecting velocity field and the forcing respectively and r is the diffusivity of the condensable substance. In the present work we shall assume the domain to be spatially bi-periodic and restrict our attention to the nondiffusive limit, $r = 0$. The problem thus consists of the advection of a passive tracer supplied by the source F , and removed by a sink associated with condensation. This sink is represented as

$$S = \begin{cases} -\frac{1}{\tau} [q - q_s(\mathbf{x})] & \text{if } q > q_s \\ 0 & \text{if } q \leq q_s \end{cases} \quad (2)$$

where $q_s(\mathbf{x})$ is the saturation mixing ratio — a prescribed function. Hence with $r = 0$, the ADC problem is closely related to the interaction of smooth advection with linear damping [8]. The ADC problem also bears a similarity to recent studies of "active" processes when coupled with fluid advection, such as the evolution of chemically [9] or biologically [10] active substances and the issue of phase separation in immiscible fluids [11].

Our aim is to examine the state of statistical equilibrium attained by (1) and (2) in the limit $\tau \rightarrow 0$ or that of rapid condensation. This limit implies that upon advection if $q(\mathbf{x};t) > q_s(\mathbf{x})$, then the parcel's mixing ratio is instantaneously reset to the saturation mixing ratio at that location. Of course, two immediately apparent opposing long time limits of (1) and (2) are: (i) Uniform forcing with $\mathbf{u} = 0$ $q(\mathbf{x};t) \rightarrow q_s(\mathbf{x})$ and (ii) A sufficiently mixing flow with $F = 0$ $q(\mathbf{x};t) \rightarrow \min_{\mathbf{x}} [q_s(\mathbf{x})]$. Hence, to achieve a non-trivial state of statistical equilibrium we require both $\mathbf{u}; F \neq 0$.

In the absence of diabatic effects, parcel motion in the midlatitude troposphere is restricted to two-dimensional surfaces of constant potential temperature, i.e. to isentropic surfaces [12]. Our objective is to understand the probability density function (PDF) of the water vapor mixing ratio along these midlatitude isentropic surfaces [13]. On average the thermal structure of the midlatitude troposphere is such that as one progresses polewards, the temperature along isentropic surfaces decreases in a fairly linear manner. Given the sensitivity of the saturation mixing ratio (via the Clausius-Clapeyron relation) to the temperature, following [7] we take q_s to vary exponentially with y . As we are in a periodic domain, $q_s(x) = q_s(y) = \exp(-\gamma(y - \frac{L}{2}))$ ($0 \leq y \leq L$) where $\gamma > 0$ and increasing γ yields progressively steeper profiles which fall off symmetrically from $y = \frac{L}{2}$. This yields an idealized model problem which retains the essence of the much more complex atmospheric problem that motivates our work. Even though the real atmosphere does not conform exactly to the idealizations, progress can be made through a detailed solution of this model problem.

II. THE PDF IN THE LIMIT OF RAPID CONDENSATION

The Liouville or transport equation satisfied by the PDF for a single realization of $\mathbf{1}$ with $\epsilon = 0$ is

$$\frac{\partial P(x; y; q; t)}{\partial t} + \frac{\partial (u_i P)}{\partial x_i} + \frac{\partial [(F + S)P]}{\partial q} = 0 \quad (3)$$

but in the limit of rapid condensation, we have $0 < q(x; y; t) < q_s(y)$. Hence (3) becomes

$$\frac{\partial P(x; y; q; t)}{\partial t} + \frac{\partial (u_i P)}{\partial x_i} + \frac{\partial (F P)}{\partial q} = 0$$

with $P(x; y; q; t) = 0$ for $q(x; y; t) > q_s(y)$ (4)

As the saturation mixing ratio is purely a function of y , if the forcing is also taken to be of the form $F = F(y)$ (in fact we will focus on the uniformly forced case) — it is reasonable to look for stationary solutions of (4) which are independent of x , i.e. $P = P(q; y)$. Of course, it is the realization of statistical equilibrium without the presence of gradient fields (as $\epsilon = 0$) that makes progress possible in the present case [4]. This circumvents the need to estimate conditional expectations of the scalar dissipation (or diffusion) which complicate advection-diffusion problems [4], [5], [16].

We now assume that the effect of the fluctuating velocity in the Liouville equation admits a diffusive representation — say by an eddy diffusivity e . This would be the case if the parcel trajectories consisted of independent Brownian motion, for example. Admittedly, this is a fairly severe assumption in that mixing by multiple scale velocity fields rarely follows a simple diffusive prescription [7]. But from a tropospheric viewpoint, it is known that the meridional (y -direction) Lagrangian eddy-velocity correlation function decays quite rapidly (on the order of a few days) [18] — hence, in this context the assumption of an eddy diffusivity may not be completely unreasonable. Note that the eddy diffusivity we refer to here is an eddy diffusivity applied to probability evolution in $(y; q; t)$ space. This is not the same as characterizing mixing by an eddy diffusivity to an evolution equation for a coarse-grained q in $(y; t)$ space. Indeed, in [7] it is shown that the Brownian model yields different coarse-grained q statistics than the mean-field diffusivity model; it is suggested further that the Brownian motion model constitutes a minimal model for investigation of the interplay of transport processes with a nonlinear sink term such as condensation. In that sense, the Brownian model is worth of study in and of itself.

For the Brownian representation (4) becomes

$$e \frac{\partial^2 P}{\partial y^2} + F(y) \frac{\partial P}{\partial q} = 0 \quad (5)$$

Substituting a separable form, i.e. $P(y; q) = A(q) B(y)$ in (5) gives

$$\frac{d \log(A(q))}{dq} = -k^2$$

$$\frac{d^2 B}{dy^2} = \frac{k^2}{e} F(y) B(y) \quad (6)$$

For uniform forcing, i.e. $F(y) = \text{constant}$ we choose the separation constant to be k^2 as $P(q; y)$ is periodic in y .

$$P(q; y) = \sum_{m=1}^{\infty} \exp(-k^2 q) [C_m \cos(y) + D_m \sin(y)]; \quad = \frac{m}{L} \quad (7)$$

which gives $k^2 = \frac{2\pi}{L}$ and in effect after choosing L the only free parameter is the ratio $\frac{m}{L}$.

To obtain PDF of q we estimate the probability that $q < Q$ as a function of Q (i.e. Q represents the sample space variable corresponding to q). As $P(q; y) = 0$ for $q(x; y; t) > q_s(y)$, $P(q; y)$ has to be integrated with respect to the saturation curve $q_s(y)$. Therefore,

$$Pr(q < Q) = \frac{I_1 + I_2}{I_t} \quad (8)$$

Here $I_1; I_2$ correspond to the regions $y < Y$ and $y > Y$ where $Y = F(Q)$ (F being the inverse of $q_s(y)$). Specifically,

$$I_1 = \int_{F(Q)}^{Z_0} \int_{q_s(y)}^{Q_2} P(q; y) dq dy$$

$$I_2 = \int_{F(Q)}^{Q_2} \int_{q_s(y)}^{Q_2} P(q; y) dq dy \quad (9)$$

where $Q_2 = m$ in q_s . I_t in (8) is the same as I_2 but with 0 as the lower limit of integration in the outer integral. Substituting for $P(q; y)$ and setting $dG_m = dy = [C_m \cos(y) + D_m \sin(y)]$ for notational simplicity,

$$I_1(m) = \frac{[\exp(-k^2 Q) + \exp(-k^2 Q_2)]}{k^2} [G_m(F(Q)) - G_m(0)] \quad (10)$$

Similarly,

$$I_2(m) = \frac{\exp(-k^2 Q_2)}{k^2} [G_m(L) - G_m(F(Q))] - \frac{X(m)}{k^2} \quad (11)$$

where

$$X(m) = \int_{F(Q)}^L \frac{dG_m(y)}{dy} \exp[-k^2 q_s(y)] dy \quad (12)$$

As I_t is independent of Q it only affects the normalization of the PDF. Hence,

$$PDF(Q) = \frac{d(I_1 + I_2)}{dQ} = \sum_{m=1}^{\infty} \exp(-k^2 Q) [G_m(F(Q)) - G_m(0)] \quad (13)$$

Substituting for $G_m(y)$

$$PDF(Q)_m = \frac{\exp(-k^2 Q)}{k^2} [f C_m \sin[F(Q)] - D_m \cos[F(Q)] + D_m g] \quad (14)$$

Substituting for $F(Q)$ (as q_s is symmetric about $y = \frac{L}{2}$ we need only consider half of the domain with $q_s = \exp(-y)$, i.e. $F(Q) = \log(Q) = y$) with $C_m; D_m = 1/8m$

$$PDF(Q) = \sum_{m=1}^{\infty} \frac{\exp(-k^2 Q)}{k^2} [f \sin[\log(Q)] - \cos[\log(Q)] + 1/g] \quad (15)$$

The dependence of the PDF on β and γ is shown in the upper and lower panels of Fig. (1) respectively. In all cases the PDF has a peak for small q , decreases exponentially for intermediate values of q and then "rolls-off" at high q .

Further, even though the principal structure of the condensable field is controlled by the saturation mixing ratio profile, the PDF in (14) is in marked contrast to what one would obtain for a fully saturated domain. For example in the saturated case we have $P(q; \gamma) = \delta(q - q_s(\gamma))$, substituting this in (9) immediately yields $\text{PDF}(Q_{\text{sat}}) = \frac{dF(Q)}{dQ}$ which implies a power law (Q^{-1}) , with no "roll-off" for high Q when $q = \exp(-\gamma)$. At first sight the roll-off in (15) appears to be an obvious result of enforcing rapid condensation, but note that the saturated case considered above also conforms with the rapid condensation limit yet it yields a very different PDF. This is illustrated more clearly by choosing $q_s(\gamma)$ to be a linearly decreasing function of γ , now the saturated PDF is uniform, whereas (14) again yields a slowly decaying PDF with a smooth roll-off at large q .

With regards to water vapor, given the logarithmic dependence of the infrared cooling on the water vapor mixing ratio, it follows that fluctuations in the mixing ratio actually increase infrared cooling [7]. Hence a slowly decaying PDF, by increasing the probability of encountering a large fluctuation (as compared to a normal PDF), increases the efficiency of radiative cooling to space. In this regard, the rapid roll-off of the tail of the PDF could play a strong role in that it sharply decreases the possibility of very large fluctuations — for example, in comparison to an advection-diffusion model of water vapor distribution where one would encounter exponential tails under homogeneous forcing [19] — and would imply a reduction in the infrared cooling or in other words an increase in the temperature of the surface to maintain energy balance. Quantifying this effect by using a full-edged atmospheric radiation code is a project we hope to pursue in the near future.

III. NUMERICAL SIMULATIONS

A primary assumption in our derivation was the use of an "eddy diffusivity" to represent the effect of an advecting velocity field on the evolution of probability. As mentioned, in most flows of interest the velocity field is expected to be quite coherent and might not conform to a diffusive representation. To test the stringency of this assumption we numerically simulate the ADC system by employing a lattice map for purposes of smooth large scale advective mixing [20], [21]. The velocity field is

$$\begin{aligned} u(x; y; t) &= f(t) A_1 \sin(B_1 y + p_n) \\ v(x; y; t) &= (1 - f(t)) A_2 \sin(B_2 x + q_n) \end{aligned} \quad (16)$$

where $A_1 = A_2 = 1; B_1 = B_2 = 2$, $f(t)$ is 1 for $nT - t < (n+1)T - 2$ and 0 for $(n+1)T - 2 - t < (n+1)T$. $p_n; q_n \in [0; 2\pi)$ are random numbers selected at the beginning of each iteration, i.e., for each period T . Advection is implemented via sequential integer shifts in the x and y directions on a square lattice (see [20] for details). Apart from its numerical efficiency the lattice map has the advantage of preserving moments, i.e. it does not introduce spurious diffusion into the problem. Opposing initial conditions, a completely dry and a fully saturated domain, are used to start the simulations with a uniform forcing applied at every iteration. Fig. (2) shows the ratio of the total substance being condensed out at every step to the forcing and the spatial average of the condensable field as a function of the iteration. As is seen both initial conditions settle into the same state of equilibrium.

To test our theoretical estimate of the PDF of q we vary β with $\beta = \min[q_s(\gamma)]$. Note that β decreases with increasing γ . A snapshot of the equilibrium condensable field for $\beta = 1.5; 2$ is shown in Fig. (3). The PDF's for the different cases can be seen in Fig. (4) — the plotted PDF's are averages over the last couple of iterations of the map. In spite of the non-local nature of the mixing protocol the shapes of the PDF's follow theoretical estimates derived under an eddy-diffusive approximation. Of course, as the advective map parameters are unchanged in the different simulations, β is the same in all cases and from Fig. (1) the slope of the PDF is expected to increase with decreasing β — which is precisely what is observed in Fig. (3).

Another measure of quantifying intermittency in a field is to examine its structure functions, defined as $S_n(\vec{x}) = \langle \int_{\vec{x}} (\vec{x} + \vec{r}) - q(\vec{x})^n \rangle$ (in the present situation $\langle \cdot \rangle$ denotes a spatial average) higher moments (i.e. larger

n) of the structure functions are most sensitive to the "roughest" regions of the field. For the condensable field, we observe that $S_n(r) \sim r^{-\alpha_n}$ for $l_1 < r < l_2$ where $l_1 \neq 0$ as we are dealing with a non-diffusive problem and l_2 is an outer scale which is smaller than the size of the domain. More to the point, the exponents α_n are anomalous in the sense $\alpha_n < \alpha_{n-1}$ for $n > 1$. In fact, we observe near saturation of the scaling exponents (i.e. α_n tends to a constant) for large n . Both the scaling of the structure functions and the extracted scaling exponents are shown in Fig. (5). The anomalous behaviour is physically anticipated as smooth advection by itself leads to the formation of sharp fronts in finite time | hence one has a field composed of smooth regions interrupted by step like discontinuities. Indeed the combination of these two structures yields a α_n profile which increases linearly for $n \leq 1$ and then saturates to a constant (i.e. extreme intermittency) for $n > 1$ [22]. As the additional presence of condensation does not involve any smoothing of the field, we do not expect it to be able to mollify the discontinuities created via advection. But rapid condensation provides a bound for the magnitude of the jump across the advective discontinuity, i.e. $|q(x+r) - q(x)| \leq \exp(-Lr)$, hence we expect a weak dependence of α_n on L . Indeed, this qualitative reasoning is borne out in the lower panel Fig. (5). In a similar vein, it has been shown (under further assumptions regarding the nature of the velocity field) that an interplay of advection with linear damping produces severe anomalous scaling [8]. Interestingly, such anomalous behaviour | with saturation of α_n for large n | has been observed in an analysis of specific humidity fluctuations from high resolution aircraft data in the troposphere [3].

Further, as is evident from (15) for a fixed flow (i.e. fixed u) the mean of the condensable field is a function of the forcing strength. In fact, as is seen in Fig. (6) | which shows the numerically computed mean as well as the mean using the first mode of (15) | the mean of the condensable field increases with the forcing strength until $\langle q \rangle = m \alpha_{q,x} [q_s(x)]$ when the entire domain becomes saturated.

IV. CONCLUSIONS AND ATMOSPHERIC DATA

We have examined the state of equilibrium achieved via the interplay of smooth advection and condensation. Exploiting the attainment of equilibrium without the presence of gradient fields allows us to make progress on the Liouville equation governing the PDF of the condensable substance. The analytically estimated PDF, derived in the limit of rapid condensation with the assumption of an eddy-diffusivity, is seen to compare favourably with numerical simulations. Even though in the present situation we are dealing with the case $\beta = 0$, the presence of a slowly decaying PDF is not entirely unexpected when taken in the context of passive advection-damping [8]. Indeed, it is the rapid "roll-off" for $q \sim m \alpha_{q,x} [q_s(x)]$ that stands out as a characteristic feature of the PDF. Further, scaling exponents extracted from structure functions of the condensable field show anomalous behaviour. Physically, the anomalous scaling is anticipated given the tendency of undisturbed smooth advection to create sharp fronts. In fact, the near saturation of α_n for large n is a reflection of these fronts providing the leading contribution to the higher order structure functions.

As mentioned in the Introduction, our motivation is to understand the distribution of water vapor along midlatitude isentropic surfaces. With this in mind we construct PDF's of the midlatitudinal specific humidity field along the 300 K isentrope using data from the ECMWF reanalysis (ERA 40) project. As is seen in Fig. (7), despite the simplifying assumptions made in our derivation, the PDF's from data bear a fair resemblance to theory. It is for large q that the PDF's from data deviate significantly from the theoretical estimate. As we have considered the nondiffusive limit a possible source of this discrepancy might lie in the homogenization induced by diffusion. Secondly, as the source of water vapor lies in the tropics a boundary forcing might be more appropriate for the actual atmospheric problem. Even so, these moderately encouraging results lead us to conjecture that the ADC model driven by idealized velocity fields might be of use in predicting the statistical properties of the large scale distribution of water vapor in the midlatitude troposphere.

Acknowledgments

We thank Prof. W. R. Young (Scripps Institute, UCSD) for his suggestions which led to a clearer formulation of the problem. J.S. would also like to acknowledge helpful conversations with Dr. A. Alexakis (NCAR). Much of this work was carried out while the first author was at the National Center for Atmospheric Research which is sponsored

by the National Science Foundation. The second author's contribution to this work was sponsored by the National Science Foundation under grant ATM -0123999.

-
- [1] G .Falkovich, K .Gawedzki and M .Vergassola, *Rev. Mod. Physics*, 73, 913 (2001).
 - [2] S.C .Sherwood, *J. Climate*, 9, 2919 (1996).
 - [3] E.P .Salathe and D.L .Hartmann, *J. Climate*, 10, 2533 (1997).
 - [4] R.T .Pierrehumbert, *Geophys. Res. Lett.* 25, 151 (1998).
 - [5] R.T .Pierrehumbert, *Nature*, 419, 191 (2002).
 - [6] I.Held and B .Soden, *Annu. Rev. Energy Environ.* 25, 441 (2000).
 - [7] R.T .Pierrehumbert, H .Brogiez and R .Roca; in *The General Circulation of the Atmosphere*, edited by T .Schneider and A .Sobel (Princeton University Press, 2005) (to appear)
 - [8] M .Chertkov, *Phys. of Fluids*, 10, 3017 (1998).
 - [9] Z.Neufeld, C .Lopez and P.H .Haynes, *Phys. Rev. Lett.* 82, 2606 (1999).
 - [10] E.R .Abraham, *Nature*, 391, 577 (1998).
 - [11] L.Berthier, J-L .Barrat and J.Kurchan, *Phys. Rev. Lett.* 86, 2014 (2001).
 - [12] B .Hoskins, *Tellus*, 43A , 27 (1991).
 - [13] H .Yang and R.T .Pierrehumbert, *J. Atmos. Sci.* 51, 3437 (1994).
 - [14] S.B .Pope, *Prog. Energy Combust. Sci.* 11, 119 (1985).
 - [15] C .Dopazo, L .Valino and N .Fueyo, *Int. Journal of Mod. Physics B*, 11, 2975 (1997);
 - [16] J.Sukhatme, *Phys. Rev. E*, 69, 056302 (2004).
 - [17] A.J .Majda and P.R .Kramer, *Physics Reports*, 314, 238 (1999).
 - [18] J.Sukhatme, *J. Atmos. Sci.* 62, 3831 (2005).
 - [19] M .Chertkov, G .Falkovich, I.Kolokolov and V .Lebedev, *Phys. Rev. E*, 51, 5609 (1995).
 - [20] R.T .Pierrehumbert, *Chaos*, 10, 1, 61 (2000).
 - [21] J.Sukhatme and R.T .Pierrehumbert, *Phys. Rev. E*, 66, 056302 (2002).
 - [22] E .Aurell, U .Frisch, J.Lusko and M .Vergassola, *J. Fluid. Mech.*, 238, 467 (1992).
 - [23] J.Cho, R .Newell and G .Sachse, *Geophys. Res. Lett.* 27, 377 (2000).
 - [24] A similar absence of gradient velds in equilibrium has been indirectly exploited in the study of advection with linear damping [8].

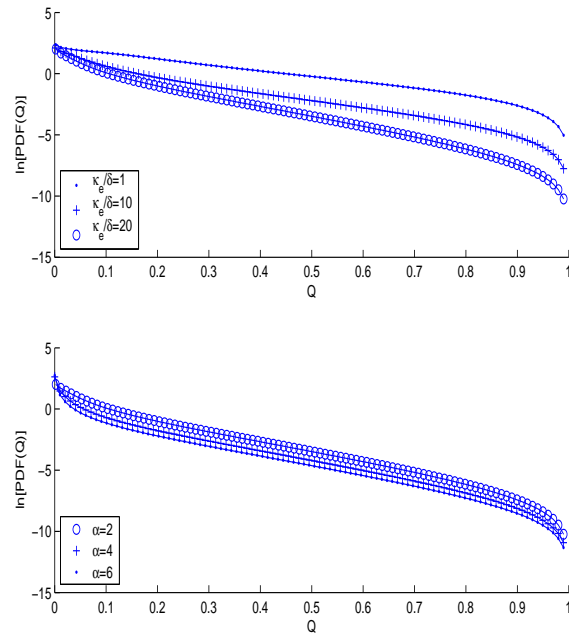


FIG .1: The PDF in (15) with $L = 2$. Upper panel : Varying β with $\alpha = 2$. Lower Panel : Varying α with $\beta = 20$.

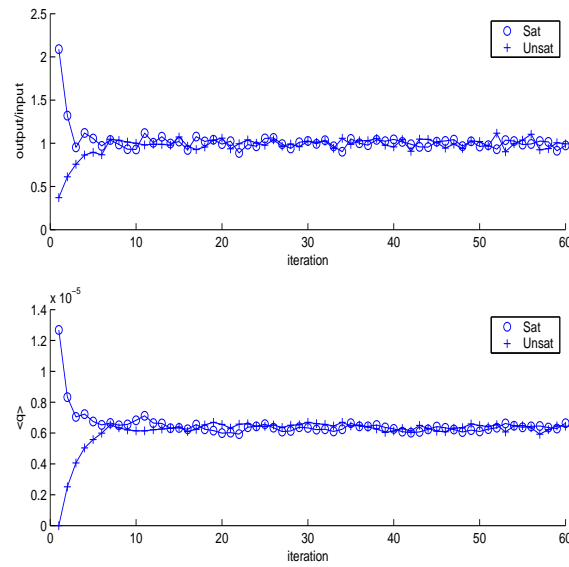


FIG .2: Upper Panel : The total amount that condenses out of the domain divided by the total input into the domain as a function of iteration. As expected this $\rightarrow 1$, i.e. we achieve a balance between the forcing and the sink, as we settle into equilibrium . Lower Panel : Spatial average of q .

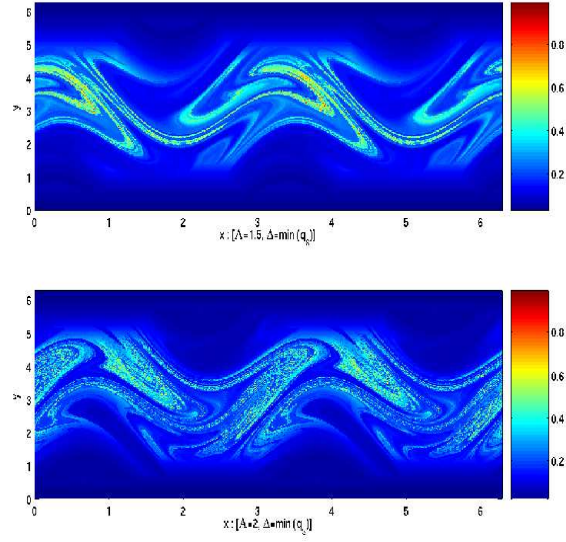


FIG .3: A snapshot of the normalized condensable field in equilibrium for $\alpha = 1.5$ and $\alpha = 2$.

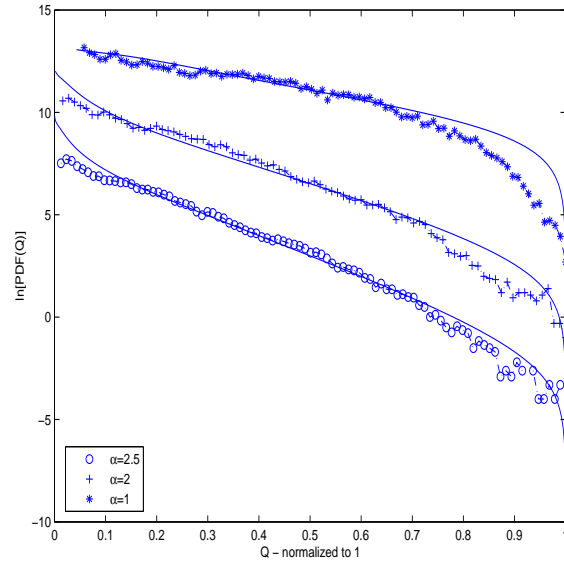


FIG .4: The PDF using the lattice map for $\alpha = 1; 2; 2.5$ with constant forcing ($\delta = \min(q_i)$). The curves have been shifted for clarity. The solid lines are plots of (15) (shifted vertically by a constant). Consistent with Fig. (1), the slope increases with decreasing forcing.

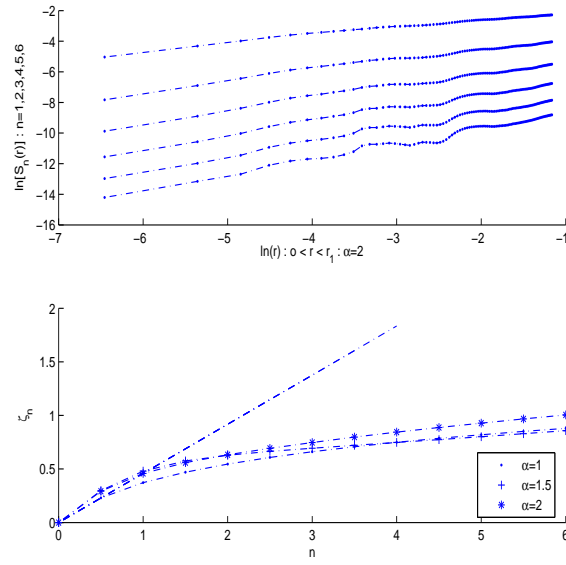


FIG .5: Upper Panel : Plots of $\log(S_q(r))$ V s. $\log(r)$ for the first six moments of the equilibrium condensable field with $\alpha = 2$. Lower panel : Scaling exponents extracted from above (for $\alpha = 2$) and similar plots (not shown) for $\alpha = 1; 1.5$.

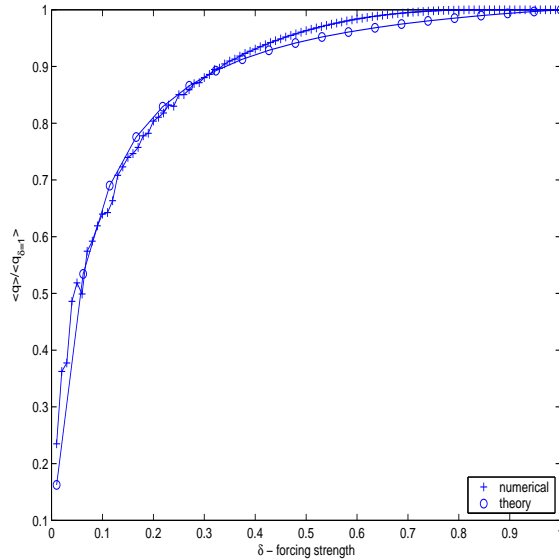


FIG .6: The effect of varying the forcing strength on $\langle q \rangle$ both numerically and using a single mode of (i.e. $m = 1$) (15) ($L = \infty$; $\epsilon = 1$). The mean of the condensable field increases with δ until $\delta = m \alpha \times [\zeta_n^c(\alpha)]$ where the domain becomes fully saturated.

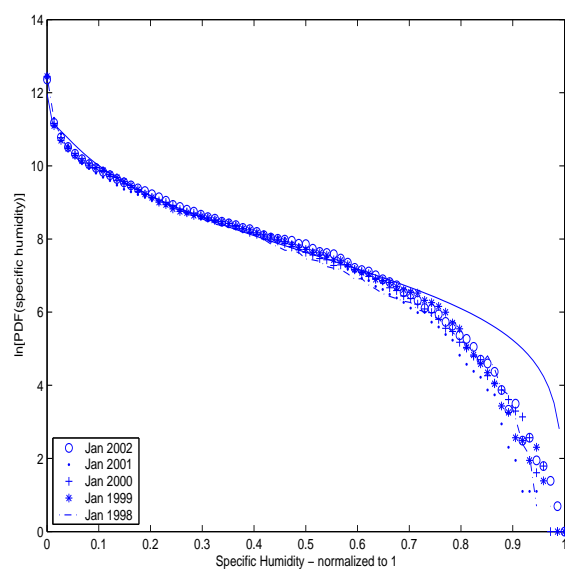


FIG. 7: The normalized specific humidity PDF's in the midlatitudes (between 30 and 60 in both hemispheres) along the 300 K isentropic surface for Jan 97-02 from ECMWF data. The solid line is a plot of (15) with $\frac{\sigma}{\sigma_0} = 2.5$; $\beta = 4$; $L = 2$